Tactile form and location processing in the human brain

Robert W. Van Boven, John E. Ingeholm, Michael S. Beauchamp, Philip C. Bikle, and Leslie G. Ungerleider†

Laboratory of Brain and Cognition, National Institute of Mental Health, National Institutes of Health, Department of Health and Human Services, Bethesda, MD 20892

To elucidate the neural basis of the recognition of tactile form and location, we used functional MRI while subjects discriminated gratings delivered to the fingertip of either the right or left hand. Subjects were required to selectively attend to either grating orientation or grating location under identical stimulus conditions. Independent of the hand that was stimulated, grating orientation discrimination selectively activated the left intraparietal sulcus, whereas grating location discrimination selectively activated the right temporoparietal junction. Hence, hemispheric dominance appears to be an organizing principle for cortical processing of tactile form and location.

brain imaging | functional MRI | somatosensory

Touch provides a rich variety of information about both the world around us and the body itself. For example, we can dissociate information about features of objects touched from knowledge of the spatial location of bodily contact. Although much is known about the peripheral mechanisms of touch, central mechanisms beyond the primary somatosensory cortex (SI) are far less well understood. In this functional MRI (fMRI) study, we aimed to dissociate the higher, central neural correlates of tactile form vs. location processing by using a selective attention task under conditions of identical peripheral stimulation.

For tactile form discrimination, we selected the grating orientation (GO) task (1), the performance of which is dependent on the spatial information conveyed by the population response of slow-adapting afferents of the peripheral nervous system (2). The information provided by this neuronal population is the basis of fine tactile form recognition used in Braille reading, texture discrimination, and other functions requiring fine spatial resolution. For grating location (GL) discrimination, we used a device to deliver small, discrete shifts in the stimulation site at which gratings were applied. By contrasting brain activations during the GO and GL tasks, we distinguished regions selectively associated with tactile form and location processing, respectively. Further, by comparing brain activations during stimulation of the right and left hands, we determined whether observed hemispheric lateralizations were a function of side of stimulation or hemispheric specialization for these perceptual attributes. We found that the regions mediating tactile form vs. location processing are distinct, lateralized, and independent of the side of the body stimulated.

Materials and Methods

Subjects. Twenty healthy subjects (11 males; mean age, 25.6 years; range, 22–28 years; 18 right-handed and 2 left-handed, according to global self-assessment) participated in this study with informed consent according to a protocol approved by the institutional review board of the National Institute of Mental Health. Eight subjects were tested at the right hand, eight at the left hand, and four at both hands (the two left-handers were tested at the right hand only).

The subjects had no history of neurological or psychiatric disorders, neurological trauma, disabling medical conditions, or brain abnormalities as evidenced by MRI and had normal neurological examinations that were performed by a neurologist.

Stimuli and Tasks. The stimuli consisted of plastic, mechanical gratings with equidistant bar and groove widths that are cut into hemispheric Johnson–Van Boven–Phillips domes (Med-Core, St. Louis). The spatial periods varied for each Johnson–Van Boven–Phillips dome. Domes were pressed onto the palmar surface of the distal phalanx of an immobilized index finger through the use of a nonmagnetic, spring-loaded fixture (Fig. 1a). During scanning, the experimenter was visually cued to manually position and release the grating when signaled by a computer-driven timing mechanism. The grating was delivered with a spring-loaded force of 1.3 ± 0.2 N orthogonal to the skin surface (measured outside the scanner). The fixture allowed passive touch discrimination to be studied and enabled controlled and reproducible stimulus presentations. The finger was immobilized through double-sided tape affixed to the dorsal aspect of the finger and floor of the fixture to prevent exploratory movements.

Before scanning, psychophysical thresholds were determined for two tasks, discrimination of GO and GL. Both tasks were constructed as match-to-sample tasks with a 1-s delay between sample and test stimuli. The two-alternative forced choice was match or nonmatch, determined pseudorandomly for each trial. Identical stimulus conditions were used for both tasks. On each trial, a sample stimulus was presented, followed by a test stimulus. During the sample presentation, the Johnson–Van Boven–Phillips dome was applied to the distal phalanx pad of an index finger with the bars and grooves parallel to the long axis of the finger. On half of the trials, the test stimulus matched the sample, on the other half, the test stimulus differed from the sample by 90° in orientation (i.e., orthogonal to the axis of the finger), by a proximal shift in location of the center of the dome (usually 1 mm), or both.

Subjects were tested initially on the GO task by using a block of 20 trials with a grating having a large spatial period (6 mm). Subsequently, dome gratings with progressively finer spatial periods were used until performance was at or below threshold levels (75% correct responses). Individual thresholds for the GO task ranged between groove/bar widths of 0.75 mm and 1.25 mm, values consistent with the literature (1). The grating size yielding the GO threshold for each individual was used for all later testing of that individual. For testing on the GL task, large shifts (3 mm) in the test stimulus location were administered, followed by decreases in the distance between sample and test location until threshold performance (75% correct responses) was achieved.
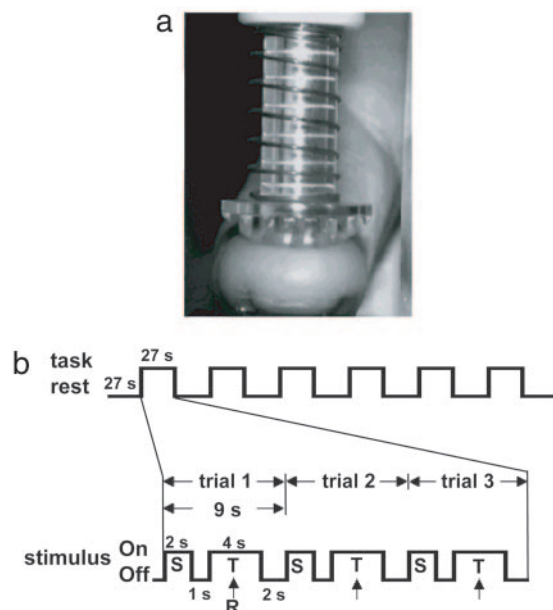
Fig. 1. Experimental apparatus and design. (*a*) Stimuli consisted of plastic, mechanical gratings (Johnson–Van Boven–Phillips domes), which were delivered to an immobilized fingertip by a spring-loaded fixture (front view of index finger shown). (*b*) During each scan series, subjects alternated between rest and task conditions (top row). Each task condition contained three trials (bottom row). During each trial, a sample stimulus (S) was presented for 2 s, followed by a 1-s delay, followed by a 4-s test stimulus (T). The subject's task was to indicate with a foot response (R) whether the test stimulus did or did not match the sample. Trial onset was cued by a yellow crosshair presented on a rear projection screen 500 ms before the sample stimulus. A gray crosshair was presented at trial onset, followed by a text cue to respond 2 s after test stimulus presentation. Subjects alternated between scan series in which they performed one of two tasks, either GO or GL; a reminder of the appropriate task was displayed on the screen at all times.

For most subjects, the GL threshold was ≈1 mm. Thresholds for two subjects were 0.5 mm. The thresholds measured for each individual during GL training were used during that subject's scanning session. Psychophysical measures were obtained for the same hand(s) used for scanning.

During MRI scanning sessions, stimulus parameters were set at the predetermined thresholds from each subject's psychometric performance such that task difficulties for the GO and GL were comparable. Subjects discriminated pairs of gratings applied to their index finger by using the same sequential two-alternative, forced-choice paradigm while lying supine inside the scanner. During the test interval, subjects were required to respond with a plantar flexion of the right foot if the test stimulus matched the sample and with a flexion of the left foot if it did not (foot responses were used in lieu of hand responses because bilateral brain activity can be induced by unilateral hand movements; responses were recorded by boots with electronic contact sensors). Each task block consisted of three trials. Each scan series (run) consisted of six alternating 27-s task and rest blocks (≈6 min; Fig. 1*b*). During each run, subjects selectively attended to either GO or GL. Subjects performed an equal number of alternating GO and GL runs (8–12 total) under identical stimulus conditions.

MRI Sessions: Data Collection and Analyses. Data were acquired with a 3.0-T GE Signa whole-body MRI system (General Electric Medical Systems, Milwaukee, WI) equipped with a head volume coil. T1-weighted spoiled gradient-recalled acquisition in steady state anatomical brain volumes (1.2-mm thickness) and standard

blood oxygen level-dependent fMRI T2*-weighted echoplanar volumes were obtained for each subject. For the echoplanar volumes, the flip angle was 90°, the echo time was 50 ms, the repetition time was 2.5 s, the in-plane resolution was 3.75×3.75 mm, and 36 3.5-mm axial slices were obtained.

Blood oxygen level-dependent fMRI data for each subject were collected in 8–12 scan runs, each run lasting 5½ min. Each run contained 132 volumes, with the first two volumes (collected before equilibrium magnetization was reached) discarded, producing an average of 1,026 brain volumes per subject.

Data were analyzed by using AFNI (3, 4). For each subject, all echoplanar volumes were registered to the volume collected closest in time to the T1 volume (5) and were spatially smoothed with a 4-mm Gaussian filter. The task-related responses were analyzed by using multiple linear regression (6). A single regressor representing each task (GO or GL) was convolved with a canonical hemodynamic response function (7). Additional regressors of no interest modeled subject head motion and linear drift within each scan series.

The overall experimental effect (both regressors of interest) thresholded at $P < 0.0001$ (uncorrected) was used to classify each voxel as "active" or "inactive". Within active voxels, the beta weights of the GO and GL regressors were compared to find voxels that showed a significant preference ($P < 0.05$) for either task. For group analysis, each individual subject was converted to the standard anatomical space of Talairach and Tournoux (8) by using AFNI. At each location in standard space, an ANOVA test was performed to compare the amplitudes of the GO and GL task responses. A mixed-effects design was used, with subject as the random factor and task as the fixed factor. The same thresholds were used for group analysis ($P < 0.0001$ for experimental effect and $P < 0.05$ for task differences). The conjunction analysis was performed by determining locations in standard space that showed the same task preference for right- and left-hand group ANOVAs, with a spatial-extent threshold of five contiguous voxels.

Because there were significant intersubject anatomical and functional differences, a region of interest (ROI)-based group analysis was also performed. An SI ROI was constructed for each subject, consisting of the postcentral gyrus just posterior to the "hand-knob" motor region (9) extending 16 mm in the superior to inferior direction. An intraparietal sulcus (IPS) ROI was constructed consisting of the IPS, extending anterior to the postcentral sulcus. Because no clear anatomical boundaries exist for temporoparietal junction (TPJ), the TPJ ROI consisted of a sphere with a radius of 17.5 mm, with the center at the posterior end of the lateral sulcus and the junction of the subject's temporal and parietal lobes [Brodmann area (BA) 40]. Within each ROI, voxels were selected that passed the overall and task thresholds (above). Counts of the number of voxels exceeding threshold were used to determine the extent of activation. The amplitude of activation in each ROI was determined by calculating the mean fMRI response from all active voxels. Individual differences between hemispheres in mean activations and task-selective voxel counts in the IPS and TPJ were analyzed by using a paired, two-tailed t test with a significance criterion set at $P < 0.05$. A nonparametric Wilcoxon rank sum test also was performed, and the results showed levels of significance comparable to those of the t test.

Results

Behavioral Data. An analysis of the behavioral data collected during MRI scanning indicated that the GO and GL tasks were challenging and of comparable difficulty. For right-hand stimulation, the mean percent correct was 79% (SE = ±5%) for the GO task and 77% (SE = ±6%) for the GL task ($P = 0.56$). For left-hand stimulation, the mean percent correct was 69% (SE = ±6%) for the GO task and 71% (SE = ±6%) for the GL task
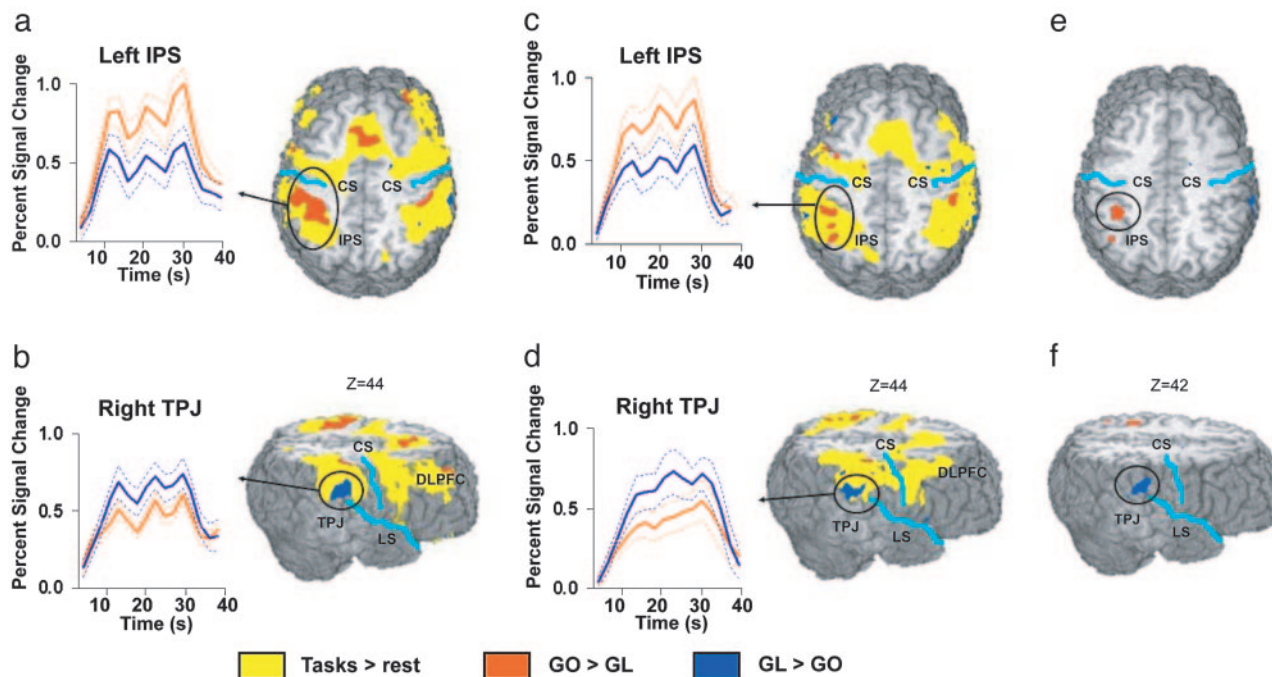
Fig. 2. Areas engaged during performance of the GO and GL tasks. Mixed-effects maps for the right-hand (*a* and *b*; *n* = 12) and left-hand (*c* and *d*; *n* = 12) stimulation groups show regions (yellow) significantly activated by both tasks vs. rest ($P < 10^{-5}$). Voxels showing a significantly greater response to one of the tasks ($P < 0.05$) are shown in orange (GO > GL) or blue (GL > GO). Maps are displayed on a rendered brain of a single subject (left is left for axial views). Graphs show the average magnetic resonance signal change (solid lines) and standard errors of the mean (dashed lines) during blocks of the GO task (orange line) and the GL task (blue line). The three peaks in each graph correspond to the three trials comprising each block (Fig. 1*b*). Black circles show the location of voxels used to calculate the average time series: GO-preferring voxels (colored orange) for IPS time series and GL-preferring voxels (colored blue) for TPJ time series. (*e* and *f*) Conjunction map of voxels showing the same task preference during both right-hand and left-hand stimulation ($P < 10^{-4}$), including IPS for GO > GL (center of mass coordinates −37, −38, 41) and TPJ for GL > GO (59, −33, 27). A GO activation site in the left premotor cortex (−37, 2, 32) is not shown. The thick, light blue lines show the location of the central sulcus and the lateral sulcus. CS, central sulcus; DLPFC, dorsolateral prefrontal cortex; IPS, intraparietal sulcus; LS, lateral sulcus; TPJ, temporoparietal junction.

($P = 0.59$). Averaged over both tasks, the mean percent was 78% (SE = ±3%) and 70% (SE = ±3%) for right-hand and left-hand stimulation, respectively, a significant difference ($P = 0.002$). Thus, although performance was better with the right hand, performances on the GO and GL tasks were comparable regardless of the hand stimulated.

There was no significant difference between subjects tested with one hand vs. those tested with both hands on either task. For the GO task, the four subjects tested with both hands scored 79% percent correct when tested with the right hand (compared with 78% for the eight subjects tested with the right hand only) and 71% correct when tested with the left hand (compared with 69% correct for the eight subjects tested with the left hand only, $P = 0.93$ and $P = 0.71$, respectively). For the GL task, the four subjects tested with both hands scored 76% percent correct when tested with the right hand (compared with 78% for the eight subjects tested with the right hand only) and 71% correct when tested with the left hand (compared with 71% correct for the eight subjects tested with the left hand only, $P = 0.58$ and $P = 0.90$, respectively).

Finally, for the GO task, right-handed subjects averaged 79% correct and the left-handed subjects averaged 77% correct ($P = 0.77$). For the GL task, right-handed subjects averaged 76% correct and the left-handed subjects averaged 85% correct ($P = 0.17$). However, with only two left-handed subjects, it is difficult to assess the reliability of this comparison.

fMRI Data. For the fMRI data, we first performed a random-effects analysis on the data for right-hand stimulation. A comparison of brain activations evoked by the tasks compared with rest (Fig. 2 *a* and *b*) revealed a number of regions known to be involved in somatosensory processing (10), attention (11), and working memory (12). These regions included contralateral SI (BA 3b, 1, and 2), ipsilateral cerebellum, and bilaterally, secondary somatosensory cortex (SII), posterior parietal cortex (BA 5 and 7), including the IPS, TPJ (BA 40), anterior cingulate cortex (BA 32), frontal operculum (BA 44), dorsolateral prefrontal cortex (BA 46), premotor cortex (BA 6), frontal eye fields (BA 8), supplementary motor area (SMA, BA 6), and globus pallidus.

Within these regions, GO resulted in greater activation relative to GL in the IPS and SMA bilaterally, left premotor cortex, contralateral SI (especially in area 2), and ipsilateral cerebellum. Although the IPS activation was bilateral, it was greater in extent and magnitude on the left (Fig. 2*a*). There were, on average, 9,047 voxels active in the left IPS and 4,660 voxels in the right IPS [$P = 0.005$; laterality index for left > right (left voxels − right voxels)/(left voxels + right voxels) = 0.32]. The mean signal change was 0.78% in the left IPS and 0.46% in the right IPS (left > right, $P < 0.0001$). In contrast, GL resulted in greater activation relative to GO in the TPJ bilaterally, although greater in extent and magnitude on the right (Fig. 2*b*). There were, on average, 4,034 active voxels in the right TPJ and 1,501 in the left TPJ ($P = 0.005$; laterality index for right > left = 0.46); the mean signal change was 0.63% for the right TPJ and 0.48% for the left TPJ (right > left, $P < 0.0001$). Hence, for right-hand stimulation, there were two striking and unexpected laterality effects: GO processing lateralized to the left IPS, and GL processing lateralized to the right TPJ. These results were found for all of the right-handers and the two left-handers tested.

We then asked whether these lateralized effects might be simply due to the side of stimulation or were actually indicative of hemispheric specialization of function. To address this issue, we examined activations produced by left-hand stimulation. An analysis of the activations evoked by the tasks, compared with rest, revealed virtually identical regions for the left-hand stimulation (Fig. 2 c and d) as was observed for the right hand (Fig. 2 a and b).

For left-hand stimulation (like right-hand stimulation), GO produced greater activation relative to GL in the IPS and SMA bilaterally, left premotor cortex, contralateral SI (especially in area 2), and ipsilateral cerebellum. As with right-hand stimulation, stimulation of the left hand produced greater left IPS activation (Fig. 2c). There were, on average, 9,078 voxels in the left IPS and 6,213 voxels in the right IPS ($P = 0.003$, laterality index for left > right = 0.19). The mean signal change was 0.71% for the left IPS and 0.65% for the right IPS (left > right, $P < 0.017$). GL resulted in greater activation relative to GO in the TPJ bilaterally. Again, the activation was greater in extent in the right TPJ (Fig. 2d), with 3,922 voxels in the right TPJ and 1,937 voxels in the left TPJ ($P = 0.008$, laterality index for right > left = 0.34). The mean signal change for GL was 0.61% for the right TPJ and 0.66% for the left TPJ, a nonsignificant difference ($P = 0.22$).

Thus, independent of side of stimulation, there was more extensive activation in the left IPS than in the right IPS for GO vs. GL processing and more extensive activation in the right TPJ than the left TPJ for GL vs. GO processing. To better characterize the coincidence in spatial location of these activations during right-hand and left-hand stimulation, we generated a conjunction map in standard space from separate ANOVAs for each stimulation group. The most prominent regions of overlap across the right-hand and left-hand groups were in the left IPS (mean signal change 0.57%; Fig. 2e) and left premotor cortex (mean signal change, 0.29%; data not shown) for GO-selective voxels and the right TPJ (mean signal change, 0.40%; Fig. 2f) for GL-selective voxels. We confirmed these results by using a repeated-measures ANOVA with hand of stimulation and task as the fixed factors and subject as the random factor. Table 1 summarizes the coordinates of the centers of mass and maxima for all regions showing significant activations.

In addition to regions that showed an fMRI signal increase during tactile discrimination, we also observed a set of regions, concentrated in medial parietal and frontal cortex, whose fMRI signal decreased during task performance relative to resting baseline. Two regions, one near the right temporal–parietal–occipital junction (border of BA 39 and BA 19; peak coordinates 47, −71, 22) and another in the right superior parietal lobule (BA 7; peak coordinates 11, −71, 50), showed a greater deactivation during GO than GL. However, all other areas were equally deactivated during both tasks, consistent with previous reports of a network of areas deactivated during any type of behavioral task (13, 14).

Discussion

Our finding that the GO task preferentially activates the IPS is consistent with the results of other recent imaging studies implicating this region in tactile form recognition (15–18), that is, the ability to discriminate object or surface features (e.g., curvature, roughness, and edges) and to resolve patterns (e.g., Braille) at the fingertips. These perceptual abilities, mediated exclusively by type 1 slow-adapting afferents innervating the skin (2), are distinct but can contribute to stereognosis, the ability to recognize objects by manipulation with the hand. Other sensory channels, such as joint afferents and muscle-spindle afferents, also contribute to stereognosis, even in cases where information from skin afferents is impoverished. To illustrate this point, one can easily identify a ball even while wearing a catcher's glove (yet

Table 1. Coordinates of centers of mass and maxima of regions with significant activations

	Center of mass			Maxima			
	x	y	z	x	y	z	t value
Right-hand group							
GO > GL							
Left IPS	−38	−41	44	−44	−26	33	5.97
Right IPS	43	−37	43	46	−33	34	4.83
SMA	−1	11	49	−2	3	58	4.49
Left premotor	−41	2	31	−39	4	29	5.04
Left SI	−38	−25	57	−43	−17	52	2.43
Right cerebellum	15	−56	−20	13	−55	−20	5.36
GL > GO							
Left TPJ	−49	−38	30	−51	−37	22	4.65
Right TPJ	59	−32	34	60	−30	23	4.89
Left-hand group							
GO > GL							
Left IPS	−41	−41	44	−41	−31	32	4.68
Right IPS	49	−39	44	53	−31	34	4.48
SMA	−2	−6	50	−5	−8	48	2.96
Left premotor	−37	−1	32	−35	3	39	5.50
Right SI	45	−24	58	54	−13	52	5.50
Left cerebellum	−18	−50	−17	−18	−50	−17	2.35
GL > GO							
Left TPJ	−56	−35	31	−56	−33	22	3.99
Right TPJ	60	−37	36	60	−35	26	4.73

be unable to resolve Braille characters). We selected the GO task to study the cortical representation of tactile form recognition because (i) its neural basis is well understood, i.e., the spatial information provided by the type 1 slow-adapting afferent population response (2, 19); (ii) the task affords a parametric investigation of human performance; and (iii) the task is passive, thereby enabling precise and reproducible stimulus control, free of confounds introduced by movement.

We also demonstrate left hemispheric dominance for tactile form recognition, independent of side of stimulation. Notably, a left-hemisphere advantage for processing fine spatial details (20) and shape discrimination (21) has been described in the visual system. Furthermore, patients with left but not right-hemisphere lesions have difficulties in perceiving local elements in a visual target stimulus (22). Thus, it is intriguing to find left-lateralized processing of fine spatial details in the somatosensory system as well.

Within SI, area 2 also is considered to be involved in tactile form processing based on both monkey lesion (23) and human neuroimaging (15–18) data, and indeed we found selective activation for form at this site. Previous work has implicated SII as playing an important role in tactile form processing as well (10). However, SII was not differentially activated for either the GO or GL tasks. Some recent studies have suggested that fine tactile form processing may involve visual cortical regions, either through visual imagery and/or multisensory integration (24–27). However, we did not find evidence of visual cortical activations for either task. Finally, we found more activation in the left premotor cortex, bilateral SMA, and ipsilateral cerebellum during GO relative to the GL task. One might argue that tactile form discrimination elicits greater motor planning for manipulation than tactile localization, which could account for the greater premotor, SMA, and cerebellar activity (28). Furthermore, the hand-independent, left-lateralized activation that we observed in premotor cortex is consistent with the report that transcranial magnetic stimulation of the left but not right premotor cortex disrupts movement selection of either hand (29).

Van Boven *et al.*

Although there have been a number of neuroimaging studies of tactile form discrimination, to our knowledge, ours is the first study of tactile localization, i.e., *where* one is being touched. In contrast to grating orientation, tactile localization preferentially engages the TPJ. Notably, we found that cortical processing for tactile localization was right-hemisphere dominant, independent of the side of stimulation, in a region that commonly produces neglect when damaged (30). In this context, it is interesting that Naito *et al.* (31) recently described right-hemisphere dominance in human area 2 of the primary somatosensory cortex during kinesthetic illusions produced by vibrotactile stimulation.

In this study, we hypothesized that the cortical substrates for tactile form and location discrimination might dissociate into ventral and dorsal pathways, respectively, based on the well characterized pathways known for visual "what" vs. "where" functions (32–34). However, this does not appear to be the case. In a recent report by Reed *et al.* (35), a tactile task of (nameable) object recognition revealed selective activations in the frontal pole (BA 9/10), motor cingulate cortex (BA 6/24/31/32), and premotor areas (BA 4/6), whereas a tactile task of allocentric spatial relations revealed activations bilaterally in superior parietal cortex (BA 7) and the precuneus (BA 7 and 19). Hence,

in the study by Reed *et al.*, both tactile tasks activated dorsal brain regions. Our study of tactile form and localization also did not reveal a dorsal/ventral dissociation, but we discovered a hemispheric lateralization effect.

Form perception in the visual system, as measured by a grating orientation discrimination task, appears to involve bilateral regions of both the ventral and dorsal streams in the visual system (36), whereas we have found that this function in the somatosensory system is lateralized to the left IPS. For localization, the location of objects in relationship to each other (extrapersonal, allocentric space) in vision is processed by bilateral dorsal, parietal areas (33). But we have found that the location of objects in contact with the skin (personal, egocentric space) is processed by a right-dominant region at the temporoparietal junction. Hence, rather than a ventral and dorsal segregation, hemispheric dominance appears to be an organizing principle for cortical processing of tactile form and location.

1. Van Boven, R. W. & Johnson, K. O. (1994) *Neurology* **44,** 2361–2366.
2. Johnson, K. O. (2002) in *Stevens' Handbook of Experimental Psychology*, eds. Pashler, H. & Yantis, S. (Wiley, New York), pp. 537–583.
3. Cox, R. W. (1996) *Comput. Biomed. Res.* **29,** 162–173.
4. Cox, R. W. & Hyde, J. S. (1997) *NMR Biomed.* **10,** 171–178.
5. Cox, R. W. & Jesmanowicz, A. (1999) *Magn. Reson. Med.* **42,** 1014–1018.
6. Friston, K. J., Holmes, A. P., Poline, J. B., Grasby, P. J., Williams, S. C., Frackowiak, R. S. & Turner, R. (1995) *NeuroImage* **2,** 45–53.
7. Cohen, M. S. (1997) *NeuroImage* **6,** 93–103.
8. Talairach, J. & Tournoux, P. (1988) *Co-Planar Stereotaxic Atlas of the Human Brain* (Thieme, New York).
9. Yousry, T. A., Schmid, U. D., Alkadhi, H., Schmidt, D., Peraud, A., Buettner, A. & Winkler, P. (1997) *Brain* **120,** 141–157.
10. Burton, H. & Sinclair, R. J. (2000) *J. Clin. Neurophysiol.* **17,** 575–591.
11. Kastner, S. & Ungerleider, L. G. (2000) *Annu. Rev. Neurosci.* **23,** 315–341.
12. Cabeza, R. & Nyberg, L. (2000) *J. Cognit. Neurosci.* **12,** 1–47.
13. Gusnard, D. A. & Raichle, M. E. (2001) *Nat. Rev. Neurosci.* **2,** 685–694.
14. McKiernan, K. A., Kaufman, J. N., Kucera-Thompson, J. & Binder, J. R. (2003) *J. Cognit. Neurosci.* **15,** 394–408.
15. Binkofski, F., Buccino, G., Posse, S., Seitz, R. J., Rizzolatti, G. & Freund, H. (1999) *Eur. J. Neurosci.* **11,** 3276–3286.
16. Bodegard, A., Geyer, S., Grefkes, C., Zilles, K. & Roland, P. E. (2001) *Neuron* **31,** 317–328.
17. Grefkes, C., Weiss, P. H., Zilles, K. & Fink, G. R. (2002) *Neuron* **35,** 173–184.
18. Stoeckel, M. C., Weder, B., Binkofski, F., Choi, H. J., Amunts, K., Pieperhoff, P., Shah, N. J. & Seitz, R. J. (2004) *Eur. J. Neurosci.* **19,** 1067–1072.
19. Van Boven, R. W. & Johnson, K. O. (1994) *Brain* **117,** 149–167.
20. Sergent, J. (1982) *J. Exp. Psychol. Hum. Percept. Perform.* **8,** 253–272.
21. Georgopoulos, A. P., Whang, K., Georgopoulos, M. A., Tagaris, G. A., Amirikian, B., Richter, W., Kim, S. G. & Ugurbil, K. (2001) *J. Cognit. Neurosci.* **13,** 72–89.
22. Delis, D. C., Robertson, L. C. & Efron, R. (1986) *Neuropsychologia* **24,** 205–214.
23. Semmes, J. & Mishkin, M. (1965) *J. Neurophysiol.* **28,** 473–486.
24. Sathian, K., Zangaladze, A., Hoffman, J. M. & Grafton, S. T. (1997) *NeuroReport* **8,** 3877–3881.
25. Amedi, A., Jacobson, G., Hendler, T., Malach, R. & Zohary, E. (2002) *Cereb. Cortex* **12,** 1202–1212.
26. Pietrini, P., Furey, M. L., Ricciardi, E., Gobbini, M. I., Wu, W. H., Cohen, L., Guazzelli, M. & Haxby, J. V. (2004) *Proc. Natl. Acad. Sci. USA* **101,** 5658–5663.
27. Merabet, L., Thut, G., Murray, B., Andrews, J., Hsiao, S. & Pascual-Leone, A. (2004) *Neuron* **42,** 173–179.
28. Winstein, C. J., Grafton, S. T. & Pohl, P. S. (1997) *J. Neurophysiol.* **77,** 1581–1594.
29. Schluter, N. D., Rushworth, M. F., Passingham, R. E. & Mills, K. R. (1998) *Brain* **121,** 785–799.
30. Halligan, P. W., Fink, G. R., Marshall, J. C. & Vallar, G. (2003) *Trends Cognit. Sci.* **7,** 125–133.
31. Naito, E., Roland, P. E., Grefkes, C., Choi, H. J., Eickhoff, S., Geyer, S., Zilles, K. & Ehrsson, H. H. (2005) *J. Neurophysiol.* **93,** 1020–1034.
32. Ungerleider, L. G. & Mishkin, M. (1982) in *Analysis of Visual Behavior*, eds. Ingle, D. J., Goodale, M. A. & Masfield, R. J. W. (MIT Press, Cambridge, MA), pp. 549–586.
33. Ungerleider, L. G. & Haxby, J. V. (1994) *Curr. Opin. Neurobiol.* **4,** 157–165.
34. Ungerleider, L. G. & Pasternak, T. (2004) in *The Visual Neurosciences*, eds. Chalupa, L. M. & Werner, J. S. (MIT Press, Cambridge, MA), pp. 541–562.
35. Reed, C. L., Klatzky, R. L. & Halgren, E. (2005) *NeuroImage* **25,** 718–726.
36. Faillenot, I., Sunaert, S., Van Hecke, P. & Orban, G. A. (2001) *Eur. J. Neurosci.* **13,** 585–596.

NEUROSCIENCE